J Solid State Electrochem (2009) 13:705–711
DOI 10.1007/s10008-008-0575-6

ORIGINAL PAPER

High-performance thin-film $Li_4Ti_5O_{12}$ electrodes fabricated by using ink-jet printing technique and their electrochemical properties

Yaomin Zhao · Guoqun Liu · Ling Liu · Zhiyu Jiang

Received: 14 February 2008 / Accepted: 28 April 2008 / Published online: 20 June 2008

Abstract $Li_4Ti_5O_{12}$ thin-film anode with high discharge capacity and excellent cycle stability for rechargeable lithium ion batteries was prepared successfully by using ink-jet printing technique. The prepared $Li_4Ti_5O_{12}$ thin film were characterized by scanning electron microscopy, transmission electron microscopy, X-ray diffraction, X-ray photoelectron spectroscopy, cyclic voltammograms, and galvanostatic charge–discharge measurements. It was found that the average thickness of 10-layer $Li_4Ti_5O_{12}$ film was about 1.7~1.8 μm and the active material $Li_4Ti_5O_{12}$ in the thin film was nano-sized about 50–300 nm. It was also found that the prepared $Li_4Ti_5O_{12}$ thin film exhibited a high discharge capacity of about 174 mAh/g and the discharge capacity in the 300th cycle retained 88% of the largest discharge capacity at a current density of 10.4 $\mu A/cm^2$ in the potential range of 1.0–2.0 V.

Keywords Ink-jet printing · Thin film · $Li_4Ti_5O_{12}$ · Lithium-ion battery

Y. Zhao (✉) · G. Liu
School of Material and Chemical Engineering,
Zhongyuan University of Technology,
Zhengzhou 450007, China
e-mail: zhaoyaomin@zzti.edu.cn

L. Liu · Z. Jiang
Department of Chemistry, and Shanghai Key Laboratory
of Molecular Catalysis and Innovative Materials,
Fudan University,
Shanghai 200433, China

Z. Jiang
e-mail: zyjiang@fudan.ac.cn

Introduction

Spinel $Li_4Ti_5O_{12}$ is well-known for its excellent electrochemical properties and has found its versatile potential applications in many fields till now. Firstly, spinel $Li_4Ti_5O_{12}$ has been demonstrated as a promising anode material for lithium-ion batteries because it has good Li-ion intercalation and de-intercalation reversibility and exhibits no structural change during charge-discharge cycling [1]. It exhibits a working potential of 1.55 V vs. Li^+/Li and its theoretical discharge capacity is 175 mAh/g [2–3].This anode, when coupled with the 4 V available cathodes such as $LiCoO_2$ [4–7] or $LiMn_2O_4$ [8–11], can provide a cell with an operating voltage of 2.5 V which is twice that of Ni/MH or Ni/Cd. Secondly, the improved safety and reliability of the spinel compared with that of carbon electrodes make the lithium-ion batteries using $Li_4Ti_5O_{12}$ material as anode suitable for electric vehicle and power storage batteries. Thirdly, it can also be used in hybrid supercapacitors by combination with active carbon or some conductive polymers just because of its superior cycleability and safety [12–16].

Meanwhile, many studies have been carried out on rechargeable lithium microbatteries because the microscale batteries will be utilized in various application fields related to microsystems, such as microsensors, micromechanics, microelectronics, and so on [17]. $Li_4Ti_5O_{12}$ in the form of thin film is also finding its potential application as anode in all solid-state lithium ion microbatteries. Many techniques such as spray pyrolysis, magnetron sputtering, electrostatic spray pyrolysis, pulsed laser deposition, soft solution processing, hydrothermal method, sol-gel method and so on have been applied to study the $LiCoO_2$ thin film cathode. By comparison, fewer techniques have been reported to investigate $Li_4Ti_5O_{12}$ thin film anode. Up to

now, thin film $Li_4Ti_5O_{12}$ has been fabricated for anode in lithium ion batteries by the following three techniques [17–21] according to some related reports as far as we know. Firstly, magnetron sputtering [18] is a typical methods for thin film preparation. C.-L. Wang et al fabricated spinel-phase $Li_4Ti_5O_{12}$ thin films by radio frequency magnetron sputtering on an Au/Ti/SiO_2/Si substrate followed by an annealing process at 500~700 °C [18]. Besides, electrostatic spray deposition [19] and spin-coating method [17, 20–21] have been also employed to obtain $Li_4Ti_5O_{12}$ thin films. Y. Yu et al reported porous thin films of $Li_4Ti_5O_{12}$ prepared by electrostatic spray deposition technique with lithium acetate and titanium butoxide as the precursors. They found that the capacity retained 150 mAh/g after 70 cycles when the heating process was carried out at 700 °C [19]. Thin films of $Li_4Ti_5O_{12}$ with a thickness of 1 μm were prepared by Y. H. Rho et al. from precursors obtained by a sol–gel process using poly(vinylpyrrolidone) followed by a heat treatment at 600–800 °C for 1 h [20].

At the same time, the application of ink-jet printing technology has been successfully extended from its traditional areas into more extensive fields such as fabrication of field-effect transistors [22–23], protein [24], high-density bacterial colony [25], even cell and organs [26] in recent years. Thin-film electrets [27] and polymer films [28] are also reported by ink-jet printing method. MnO_2 thin film electrode for primary battery and SnO_2 thin film electrode for rechargeable lithium ion batteries have been introduced in our previous papers [29–30]. Since ink-jet printing technique has many advantages such as simple device, low-cost, and facile fabrication process, ease of mass fabrication and so on, it is finding increasing application fields and a more promising future is on its way. Here, we reported $Li_4Ti_5O_{12}$ thin film electrode successfully fabricated by a simple ink-jet printing technique. The prepared $Li_4Ti_5O_{12}$ thin film electrode displayed high discharge capacity and excellent cycle stability.

Experimental

Preparation of $Li_4Ti_5O_{12}$ ink

The specific preparation process of $Li_4Ti_5O_{12}$ ink is very similar to our previous work, as shown in Fig. 1 [30]. Prior

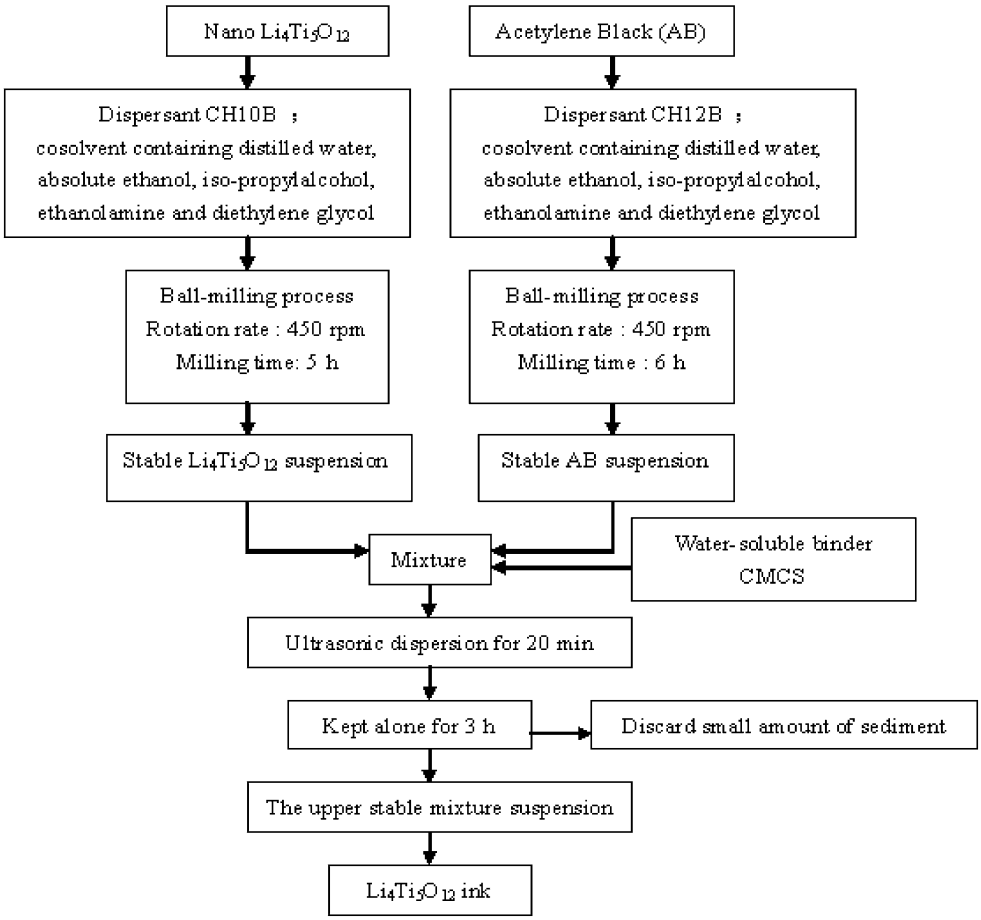

Fig. 1 Flow chart showing preparation of $Li_4Ti_5O_{12}$ ink for subsequent ink-jet printing process

to the $Li_4Ti_5O_{12}$ ink preparation, the electrochemically active $Li_4Ti_5O_{12}$ was home-made by solid-state reaction process aided with a wet-ball milling process (powder $Li_4Ti_5O_{12}$ for short hereafter). Then the ink solution was prepared as follows: firstly, $Li_4Ti_5O_{12}$ suspension was prepared by adding 50 mg polymeric hyperdispersant CH10B (Shanghai Sanzheng Polymer Material Co. Ltd) in 10 ml mixture solvent (distilled water/absolute ethanol/diethylene glycol/triethanolamine/isopropylalcohol=56:18:5:1:1 by mass ratio) and then followed by addition of 400 mg $Li_4Ti_5O_{12}$ powder. The obtained mixture was ball-milled at 450 rpm for 6 h and then the stable $Li_4Ti_5O_{12}$ suspension was achieved. The other kind of polymeric hyperdispersant CH12B (Shanghai Sanzheng Polymer Material Co. Ltd) was employed to disperse the conductive agent acetylene black (AB). Following the same procedure, CH12B 100 mg was dissolved in

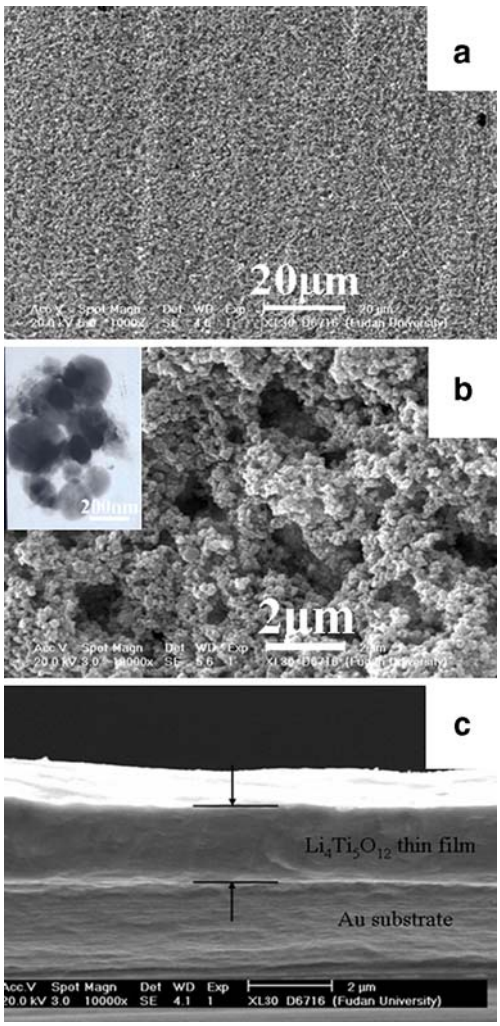

Fig. 2 SEM images for $Li_4Ti_5O_{12}$ thin films on Au substrate annealed at 550 °C for 90 min. **a** surface view with low magnification (×1000); **b** a cross-sectional view; **c** surface view with high magnification (×10,000), *Inset* is TEM image for nano-sized $Li_4Ti_5O_{12}$ in the thin film

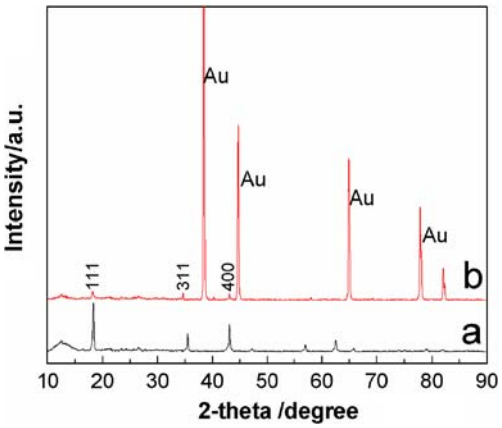

Fig. 3 X-ray diffraction patterns of *a* powder $Li_4Ti_5O_{12}$ and *b* the as-prepared $Li_4Ti_5O_{12}$ thin film annealed at 550 °C for 90 min

10-ml mixture solvent and then followed by addition of 40 mg AB. The as-prepared mixture was ball-milled at 450 rpm for 6 h and then the stable AB suspension was attained. Finally, the stable suspension $Li_4Ti_5O_{12}$ and the stable suspension AB were mixed by a certain volume ratio and then about 5% water-soluble sodium of carboxymethyl cellulose (CMCS) was added as binder, which did not destroy the stability of the dispersion system. Then the mixture suspension containing $Li_4Ti_5O_{12}$, AB, and CMCS was ultrasonically dispersed for 20 min, kept alone for 3~5 h, discarded small amount of sediment at the bottom and finally the upper stable part formed the print suspension named as $Li_4Ti_5O_{12}$ ink.

Preparation of thin film $Li_4Ti_5O_{12}$ electrodes

The $Li_4Ti_5O_{12}$ ink 10~15 ml was transferred into a well-cleaned black Canon BC-03 cartridge and then ink-jet printed through Canon 1000SP printer onto Au substrate followed by an annealing process at 550 °C for 90 min according to the pre-designed electrode size and shape. In our experiment, we repeated the printing process ten times in order to achieve enough capacity for subsequent electrochemical measurements. The as-printed $Li_4Ti_5O_{12}$ films were dried under infrared light at 80 °C for 2 h, compressed at 5 MPa, annealed at 550 °C for 90 min (as-prepared $Li_4Ti_5O_{12}$ thin film for short hereafter) and finally used for the subsequent characterization and measurements.

Characterizations

The morphology and thickness of $Li_4Ti_5O_{12}$ film were examined by means of scanning electron microscopy (SEM, Philips XL 30) and transmission electron microscopy (TEM, Joel JEM 2010). X-ray diffraction (XRD) and X-ray photoelectron spectroscopy (XPS)) were employed to

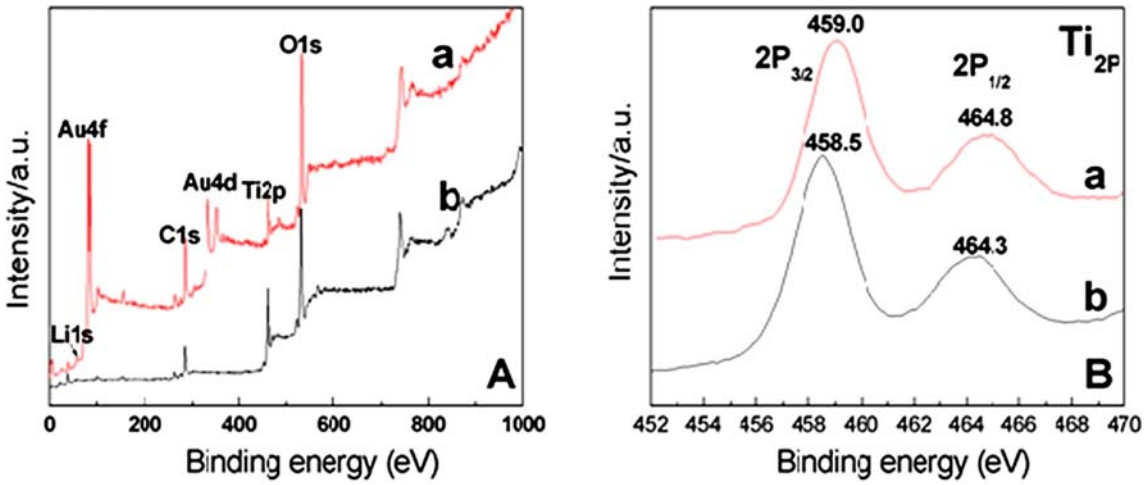

Fig. 4 XPS survey spectra (**A**) and the Ti2p region (**B**); *a* $Li_4Ti_5O_{12}$ thin film on Au substrate annealed at 550 °C for 90 min; *b* powder $Li_4Ti_5O_{12}$ home-made by solid state reaction process

investigate the structure and composition of as-prepared $Li_4Ti_5O_{12}$ thin film. XRD patterns were recorded on a Bruker D8 advanced diffractometer with Cu Kα radiation, operated at 40 mA and 40 kV. Cyclic voltammograms (CV) and galvanostatic charge–discharge measurements were performed on a CHI660 electrochemical workstation (CHI, USA) with conventional three-electrode cell. Two lithium plates were used as both the reference and counter electrode. All the electrodes were dried under vacuum at 90 °C for 12 h before they were constructed in a dry-air filled box. One molar $LiPF_6$ in ethyl carbonate (EC) and dimethyl carbonate (DMC) (EC, DMC=1:1 by volume) was used as the electrolyte. CV measurements were conducted at different sweep rates over the potential range of 1.0–2.0 V. Galvanostatic charge–discharge measurements were performed over the potential range of 1.0–2.0 V. The exact mass of $Li_4Ti_5O_{12}$ in the thin films was obtained as follows: firstly, the as-prepared thin-film was assembled into three-electrode glass cell for charge–discharge measurements. When the measurements were finished, the cells were disassembled. The $Li_4Ti_5O_{12}$ content in the thin film was determined by inductively coupled argon plasma (ICP) method (IRIS Intrepid, Thermo Elemental Company) after the sample was solubized in concentrated HNO_3–HCl solution. The mass of $Li_4Ti_5O_{12}$ was calculated on the basis of the mass of titanium achieved by ICP result.

Results and discussion

Electron micrographs of as-prepared $Li_4Ti_5O_{12}$ thin films on Au substrate are presented in Fig. 2. It can be seen that the distribution of $Li_4Ti_5O_{12}$ thin film is very uniform (Fig. 2a) and the particles are nano-sized (Fig. 2b). TEM image of $Li_4Ti_5O_{12}$ particles in the thin film (inset in Fig. 2b) shows that the particle size of nano-sized $Li_4Ti_5O_{12}$ ranges from 30~300 nm. The cross-sectional view of the as-prepared $Li_4Ti_5O_{12}$ thin films on Au substrate reveals that the average thickness of 10-layer film is about 1.7~1.8 μm, which was used for subsequent electrochemical measurements.

The X-ray diffraction of as-prepared $Li_4Ti_5O_{12}$ thin film (b) is similar to that of powder $Li_4Ti_5O_{12}$ (a) are shown in Fig. 3. The main diffraction peaks of $Li_4Ti_5O_{12}$ (111, 311.400) are indexed based on a face-centered cubic spinel structure with an Fd3m space group, which is in good agreement with the JCPDS reference (26–1198) and corresponds to typical pure-phased spinel structure [31–32]. In addition, the peaks attributed to the substrate Au for as-prepared $Li_4Ti_5O_{12}$ thin films are also clearly observed and indexed.

The survey XPS spectra corresponding to $Li_4Ti_5O_{12}$ thin film on Au substrate annealed at 550 °C for 90 min (a) and

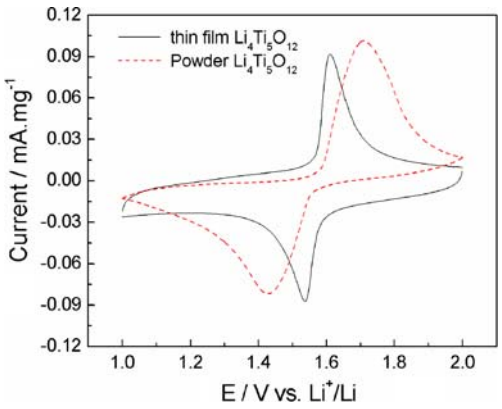

Fig. 5 Comparison of cyclic voltammograms at a scan rate of 0.1 mV/s in a mixed solvent of ethylene carbonate and dimethyl carbonate containing 1.0 mol/dm^3 $LiPF_6$ between as-prepared $Li_4Ti_5O_{12}$ thin film electrode and powder $Li_4Ti_5O_{12}$ electrode

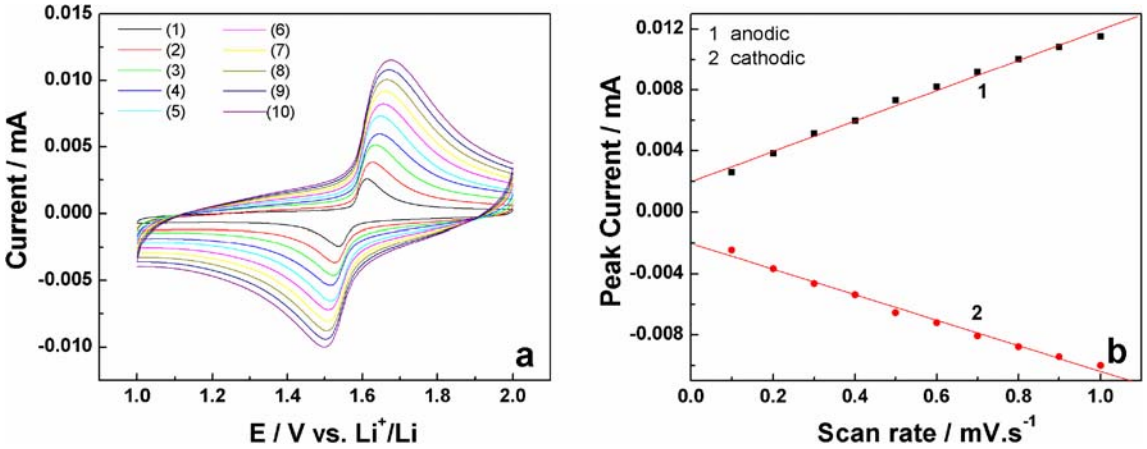

Fig. 6 **a** Cyclic voltammograms of as-prepared $Li_4Ti_5O_{12}$ thin film electrode at different scan rates of (1) 0.1, (2) 0.2, (3) 0.3, (4) 0.4, (5) 0.5, (6) 0.6, (7) 0.7, (8) 0.8, (9) 0.9, (10) 1.0 mV/s in a mixed solvent of ethylene carbonate and dimethyl carbonate containing 1.0 mol/dm^3 $LiPF_6$; **b** anodic and cathodic peak current as a function of scan rate

powder $Li_4Ti_5O_{12}$ (b) are presented in Fig. 4a. The Ti2p, O1s, and Li1s photoelectron peaks are clearly observed. Carbon peaks present in the spectra of powder $Li_4Ti_5O_{12}$ are attributed to a thin contamination layer whereas that in the as-prepared $Li_4Ti_5O_{12}$ thin film comes from conductive agent AB, the polymeric dispersants CH10B, CH12B and the binder CMCS. The high resolution spectra of the Ti2p corresponding to both the as-prepared $Li_4Ti_5O_{12}$ thin film (a) and powder $Li_4Ti_5O_{12}$ (b) are shown in Fig. 4b. The spectrum corresponding to $Li_4Ti_5O_{12}$ thin film in Fig. 4b (a) is characterized by a main doublet composed of two symmetric peaks situated at Eb ($Ti2p_{3/2}$)=459.0 eV and Eb ($Ti2p_{1/2}$)=464.8 eV. This main doublet is assigned to titanium in the IV oxidation state. In addition, it is necessary to take into account the difference between the two samples. The binding energy for $Li_4Ti_5O_{12}$ thin film increased about 0.5 eV compared with powder $Li_4Ti_5O_{12}$. The main reason for this phenomenon is the particle size difference. Powder $Li_4Ti_5O_{12}$ was prepared by solid state reaction process and composed of both nano-sized and micro-sized particles whereas $Li_4Ti_5O_{12}$ thin film was composed of only nano-sized particles ranged from 30–300 nm shown in Fig. 3. The $Li_4Ti_5O_{12}$ particles with larger size than 300 nm are not effectively dispersed during the ink preparation and therefore do not exist in the as-prepared thin film.

Figure 5 shows CV curves of as-prepared $Li_4Ti_5O_{12}$ thin film electrode compared with $Li_4Ti_5O_{12}$ powder at a scan rate of 0.1 mV/s in a mixed solvent of ethylene carbonate and dimethyl carbonate containing 1.0 mol/dm^3 $LiPF_6$. Two sharp redox peaks for $Li_4Ti_5O_{12}$ thin film were observed at 1.55 and 1.60 V vs. Li^+/Li for cathodic and anodic scans respectively, which indicates that as-prepared $Li_4Ti_5O_{12}$ thin film exhibits a typical behavior for two-phase reaction

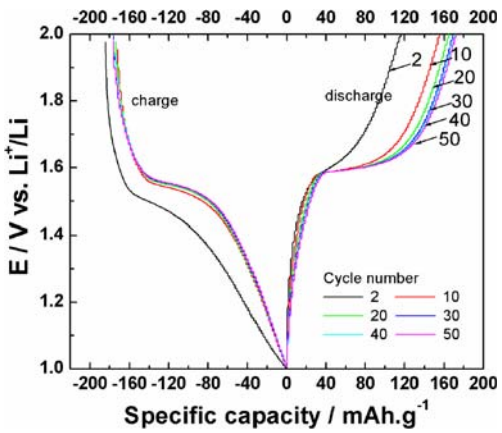

Fig. 7 Discharge and charge curves of $Li_4Ti_5O_{12}$ film prepared on Au substrate annealed at 550 °C for 90 min at a current density of 10.4 μA/cm^2 in a mixed solvent of ethylene carbonate and dimethyl carbonate containing 1.0 mol/dm^3 $LiPF_6$

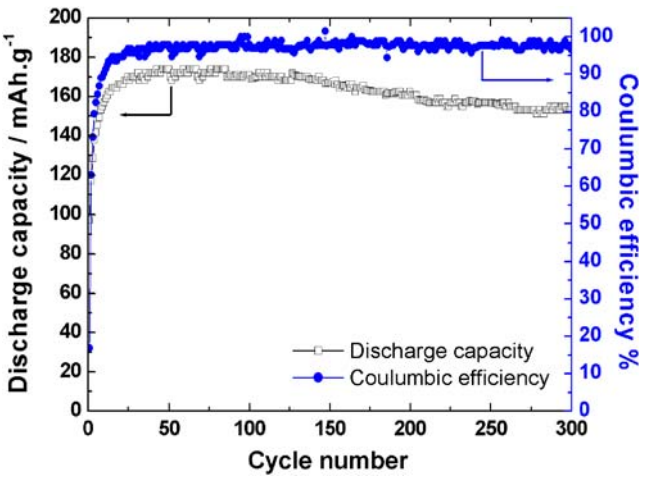

Fig. 8 Discharge capacity and coulumbic efficiency of as-printed thin film $Li_4Ti_5O_{12}$ electrode as a function of cycle number during the first 300 cycles at a constant discharge current density of 10.4 μA/cm^2 in potential range of 1.0–2.0 V

during Li^+ ion extraction and insertion processes [11, 22–23]. It can be also clearly found that the redox peaks were sharper and the peak separation was smaller for as-prepared $Li_4Ti_5O_{12}$ thin film compared with those for powder $Li_4Ti_5O_{12}$ electrode.

CV curves of $Li_4Ti_5O_{12}$ thin film on Au substrate annealed at 550 °C for 90 min at different scan rates from 0.1 to 1.0 mV/s are shown in Fig. 6a. Accordingly, the anodic and cathodic peak current as a function of scan rate are presented in Fig. 6b. It can be seen from Fig. 6 that the anodic and cathodic peak separation was 74 mV when the scan rate was 0.1 mV/s for as-prepared $Li_4Ti_5O_{12}$ thin film. The peak separation increases slightly with the increase of scan rate. The anodic peaks show a positive shift from 1.625 to 1.676 V (64 mV shifted) versus Li^+/Li with the increase of scan rate from 0.1 to 1.0 mV/s. It is easy to understand that the peak shift with the increasing scan rate was caused by the polarization of charge transfer reaction. The peak current is linearly dependent on the sweep rate, which indicates that the diffusion of lithium ion inside the electrode is not the dominating factor for as-prepared $Li_4Ti_5O_{12}$ electrode. The charge transfer process is the rate-determining step. This phenomenon is characteristic of thin film electrode.

Figure 7 shows discharge–charge curves in the second, tenth, 20th, 30th, 40th, and 50th cycle of $Li_4Ti_5O_{12}$ film prepared on Au substrate annealed at 550 °C for 90 min at a current density of 10.4 μA/cm^2 in a mixed solvent of ethylene carbonate and dimethyl carbonate containing 1.0 mol dm^{-3} $LiPF_6$. On one hand, the shape of charge-discharge curves of the as-prepared $Li_4Ti_5O_{12}$ film is similar to that of powder $Li_4Ti_5O_{12}$, which indicates the as-prepared $Li_4Ti_5O_{12}$ film has the same charge-discharge mechanism as powder $Li_4Ti_5O_{12}$ electrode. On the other hand, the charge-discharge behavior for as-prepared $Li_4Ti_5O_{12}$ thin film is very different from powder $Li_4Ti_5O_{12}$ electrode. An electrochemical activation process existed in as-prepared $Li_4Ti_5O_{12}$ films annealed at 550 °C for 90 min. The discharge capacity is small during the first several cycles and increases with the cycle process are carried through. The discharge capacity in the second, tenth, 20th, 30th, 40th, and 50th cycle of as-prepared $Li_4Ti_5O_{12}$ film is 117, 157, 166, 170, 172 and 174 mAh/g respectively. The reason for this phenomenon is not clear yet and further investigation is required.

Figure 8 displays the specific discharge capacity and coulumbic efficiency of as-prepared $Li_4Ti_5O_{12}$ thin film annealed at 500 °C for 90 min as a function of cycle number during the first 300 cycles at a constant current density of 10.4 μA/cm^2 in potential range of 1.0–2.0 V versus Li^+/Li. The initial discharge capacity is 97 mAh/g, but the discharge capacity increases with the process of cycling and the discharge capacity in the 42nd cycle reaches 174 mAh/g, which is almost near the theoretical value of spinel $Li_4Ti_5O_{12}$ material (175 mAh/g). The discharge capacity in the 300th cycle (153 mAh.g^{-1}) is 88% of the largest discharge capacity, which shows the excellent cycle stability of as-prepared $Li_4Ti_5O_{12}$ thin films. The initial coulumbic efficiency is 16.8% and the efficiency also increases with the increase of cycle number. The coulumbic efficiency maintains 98% or so after the 30th cycle. With regard to the irreversible capacity of $Li_4Ti_5O_{12}$ thin film during the first several cycles, it can be mainly attributed to parasitic cathodic reactions due to enhanced adsorption of reducible impurities such as humidity and the quality of the spinel crystalline lattice itself [2].

Conclusion

In this work, $Li_4Ti_5O_{12}$ thin films on Au substrate fabricated by using ink-jet printing technique followed by an annealing process at 550 °C for 90 min as an anode for rechargeable lithium ion batteries were investigated in detail. The as-prepared $Li_4Ti_5O_{12}$ thin films annealed at 550 °C for 90 min displayed its largest discharge capacity about 174 mAh/g. The discharge capacity in the 300th cycle (153 mAh g^{-1}) is 88% of the largest discharge capacity. The excellent electrochemical properties of the as-prepared $Li_4Ti_5O_{12}$ thin films suggest the promising application of ink-jet printing technique to thin film electrodes for lithium ion batteries.

Acknowledgements This work was supported by the National Nature Science Foundation of China; Key Youth Teacher Foundation of Zhongyuan University of Technology.

References

1. Zaghib K, Armand M, Gauthier M (1998) J Electrochem Soc 145:3135
2. Kavan L, Procházka J, Spitler TM, Kalbáč M, Zukalová M, Drezen T, Grätzelc M (2003) J Electrochem Soc 150:A1000
3. Shen C, Zhang X, Zhou Y, Li H (2002) Mater Chem Phys 78:437
4. Brousse T, Fragnaud P, Marchand R, Schleich DM, Bohnke O, West K (1997) J Power Sources 68:412
5. Jansen AN, Kahaian AJ, Kepler KD, Nelson PA, Amine K, Dees DW, Vissers DR, Thackeray MM (1999) J Power Sources 81–82:902
6. Wang Q, Zakeeruddin SM, Exnar I, Gratzela M (2004) J Electrochem Soc 151:A1598
7. Pasquier AD, Plitz I, Gural J, Badway F, Amatucci GG (2004) J Power Sources 136:160
8. Peramunage D, Abraham KM (1998) J Electrochem Soc 145:2615
9. Birke P, Salam F, Doring S, Weppner W (1999) Solid State Ionics 118:149
10. Prosini PP, Mancini R, Petrucci L, Contini V, Villano P (2001) Solid State Ionics 144:185

11. Reale P, Panero S, Scrosati B (2005) J Electrochem Soc 152: A1949
12. Amatucci GG, Badway F, Pasquier AD, Zheng T (2001) J Electrochem Soc 148:A930
13. Pasquier AD, Laforgue A, Simon P, Amatucci GG, Fauvarqueb J (2002) J Electrochem Soc 149:A302
14. Pasquier AD, Plitz I, Gural J, Menocal S, Amatucci G (2003) J Power Sources 113:62
15. Pasquier AD, Plitz I, Menocal S, Amatucci G (2003) J Power Sources 171:171
16. Pasquier AD, Laforgue A, Simon P (2004) J Power Sources 125:95
17. Rho Y, Kanamura K (2004) J Electrochem Soc 151:A106
18. Wang CL, Liao YC, Hsu FC, Tai NH, Wu MK (2005) J Electrochem Soc 152:A653
19. Yu Y, Shui JL, Chen CH (2005) Solid State Commun 135:485
20. Rho YH, Kanamura K, Fujisaki M, Hamagami J, Suda S, Umegaki T (2002) Solid State Ionics 151:151
21. Rho YH, Kanamura K (2003) J Electroanal Chem 559:69
22. Ridley BA, Nivi B, Jacobson JM (1999) Science 286:746
23. Stutzmann N, Friend RH, Sirringhaus H (2003) Science 299:1881
24. MacBeath G, Schreiber SL (2000) Science 289:1760
25. Xu T, Petridou S, Lee EH, Roth EA, Vyavahare NR, Hickman JJ, Boland T (2004) Biotechnol Bioeng 85:29
26. Wilson WC, Boland T (2003) Anat Rec A 272A:491
27. Jacobs HO, Whitesides GM (2001) Science 291:1763
28. Tekin E, de Gans B, Schubert US (2004) J Mater Chem 14: 2627
29. Xu F, Wang T, Li W, Jiang Z (2003) Chem Phys Lett 375:247
30. Zhao Y, Zhou Q, Liu L, Xu J, Jiang Z (2006) Electrochim Acta 51:2639
31. Hao Y, Lai Q, Liu D, Xu Z, Ji X (2005) Mater Chem Phys 94:382
32. Hao Y, Lai W, Xu Z, Liu X, Ji X (2005) Solid State Ionics 176:1201